Fuel 106 (2013) 271–278

Contents lists available at SciVerse ScienceDirect

Fuel

journal homepage: www.elsevier.com/locate/fuel

Modeling of soot formation during partial oxidation of producer gas

Helena Svensson [a,*], Per Tunå [a], Christian Hulteberg [a], Jan Brandin [b]

[a] Department of Chemical Engineering, Lund University, P.O. Box 124, SE-221 00 Lund, Sweden
[b] Bioenergy Technology, Linnaeus University, SE-351 95 Växjö, Sweden

HIGHLIGHTS

- Modeling of a reverse flow partial oxidation reactor for reforming.
- Study of soot formation for reforming of a gasifier product gas.
- CO and CO_2 content of gas has great influence on soot formation.
- Reduction of tars in incoming gas significantly reduces soot formation.

ARTICLE INFO

Article history:
Received 2 February 2012
Received in revised form 12 October 2012
Accepted 23 October 2012
Available online 12 November 2012

Keywords:
Gasification
Reforming
Partial oxidation
Reverse-flow operation
Synthesis gas

ABSTRACT

Soot formation in a reverse-flow partial-oxidation reactor for reforming of gasifier producer gas has been studied. The process was modeled using a detailed reaction mechanism to describe the kinetics of soot formation. The numerical model was validated against experimental data from the literature and showed good agreement with reported data. Nine cases with different gas compositions were simulated in order to study the effects of water, hydrogen and methane content of the gas. The CO and CO_2 contents, as well as the tar content of the gas, were also varied to study their effects on soot formation. The results showed that the steam and hydrogen content of the inlet gas had less impact on the soot formation than expected, while the methane content greatly influenced the soot formation. Increasing the CO_2 content of the gas reduced the amount of soot formed and gave a higher energy efficiency and methane conversion. In the case of no tar in the incoming gas the soot formation was significantly reduced. It can be concluded that removing the tar in an energy efficient way, prior to the partial oxidation reactor, will greatly reduce the amount of soot formed. Further investigation of tar reduction is needed and experimental research into this process is ongoing.

1. Introduction

The need to replace liquid fuels, such as gasoline and diesel, produced from crude oil resources has given rise to much research in the area of biofuels. Examples of liquid biofuels are ethanol, methanol and bio-diesel produced from different types of biomass using various technologies. Fischer–Tropsch diesel produced from synthesis gas (CO and H_2) derived from renewable resources is a growing area of research [1–4].

Traditionally, the synthesis gas used for the Fischer–Tropsch process was produced via coal gasification. Recently, research has been focused on the production of synthesis gas utilizing gas produced by biomass gasification [4–10]. The gas produced by the gasifier is often referred to as producer gas. This producer gas contains CO, CO_2, H_2 and H_2O, as well as CH_4 and higher hydrocarbons, including some tar compounds. There are also small amounts of contaminants present in the syngas, such as NH_3, H_2S, COS and HCN. The composition of the producer gas and the range and amounts of contaminants is largely dependent on the type of biomass and gasifier used for the production of the producer gas.

In order to upgrade the producer gas to synthesis gas, which can be used e.g. to produce liquid fuels, a reforming process is necessary. Many alternatives are available and have been the subject of much research, such as steam reforming, autothermal reforming, and catalytic partial oxidation. The main problem associated with these techniques is that they rely on catalysts that are highly susceptible to sulfur poisoning [11–14]. Although much research has been devoted to finding suitable catalysts for these techniques no clear alternative has yet emerged. An alternative would be to use a non-catalytic process such as partial oxidation (POX). One drawback associated with POX is the high temperature needed to reform methane. This results in a process with a lower energy efficiency than the catalytic alternatives and a loss of chemically

* Corresponding author. Tel.: +46 46 222 9313; fax: +46 46 14 91 56.
E-mail addresses: helena.svensson@chemeng.lth.se (H. Svensson), per.tuna@chemeng.lth.se (P. Tunå), christian.hulteberg@chemeng.lth.se (C. Hulteberg), jan.brandin@lnu.se (J. Brandin).

0016-2361/$ - see front matter © 2012 Elsevier Ltd. All rights reserved.
http://dx.doi.org/10.1016/j.fuel.2012.10.061

bound energy in the gas. One way of making the process more energy efficient is to use a reverse-flow POX reactor. The reverse-flow reactor consists of a vessel filled with an inert granular material with high thermal capacity, which acts as a heat buffer. As the gas flows through the packed bed, heat produced by the reactions is transferred from the gas to the stationary phase. When the flow direction is reversed the heat stored in the bed is used to heat the incoming cold gas. Eventually, a pseudo-steady-state temperature profile is established with a high temperature in the middle of the reactor and lower temperatures at the inlet and outlet. This concept has been studied previously and has proven highly effective for reforming hydrocarbon fuels [15–17].

The reverse-flow POX reactor has been modeled in previous work, showing potential in dealing with the unique qualities of the producer gas that make it difficult to reform using conventional techniques [18]. However some issues still remain to be resolved. Because of the high temperature required for POX, and the general composition of the producer gas, soot is likely to form during reforming. Furthermore, soot precursors, such as ethylene, acetylene and tars, are present in the producer gas promoting soot formation [19–21]. Since the reverse-flow reactor consists of a packed bed it is vulnerable to blockage if too much soot is formed.

In order to evaluate the ability of the reverse-flow POX reactor to reform producer gas, it is of the utmost importance to establish how much of the incoming carbon is likely to be converted into soot, and explore ways of reducing the formation of soot, while maintaining an energy efficient process and high methane conversion. Because of the inherent difficulties in measuring and analyzing the soot formed in different parts of the reactor, modeling of the process was undertaken as a first step in this investigation. The aim of the investigation was to examine the extent to which soot is likely to form and possible ways of counteracting such formation. The results were evaluated from the viewpoint of synthesis gas energy efficiency and methane conversion, as well as soot reduction.

2. Modeling

The reverse-flow POX reactor is an example of a forced unsteady-state system due to the reversal of flow direction during operation. The system consists of a reactor filled with a granular material with high thermal capacity that acts as a heat buffer. As the gas flows through the packed bed, heat produced by the reactions is transferred from the gas to the stationary phase. When the flow direction is reversed, the heat stored in the bed is used to heat the incoming cold gas. Eventually a pseudo-steady-state temperature profile is established with a high temperature in the middle of the reactor while the inlet and outlet are kept at a lower temperature. A depiction of the modeled system is given in Fig. 1. When the incoming gas flow is introduced in the top of the reactor the reformed gas exits at the bottom. When the flow direction is reversed the reformed gas exits at the top of the reactor. The dimensions of the modeled reverse flow reactor are given in Table 1.

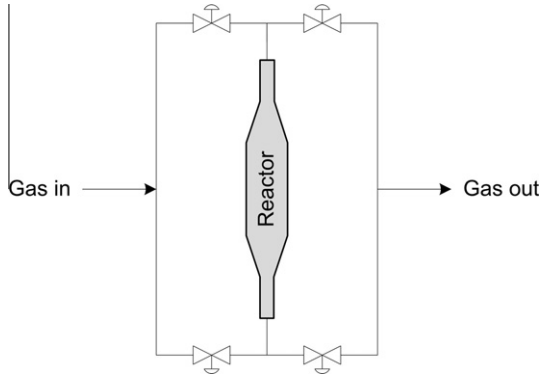

Fig. 1. Modeled reactor system with four valves to reverse the flow direction through the reactor.

In order to model a forced unsteady-state system, such as the reverse-flow reformer, the dynamic behavior needs to be described within the model. However, in order to capture the dynamic behavior the model needs to be very extensive. In order to study the soot formation in the reverse-flow reformer a very extensive reaction mechanism is needed to describe the growth to soot. Because a more detailed reaction mechanism is needed to describe the soot formation the model describing the reverse flow reformer has to be simplified, otherwise the numerical model will be unable to converge and find a solution.

Within the work on the reverse flow reformer conducted at the Department of Chemical Engineering at Lund University, a detailed numerical model of the reverse-flow reactor, designed to accurately describe the dynamic behavior of the reactor, has been developed and previously reported [18]. A brief description of the dynamic model will be given in Section 2.1. A simplified description of the reverse flow reformer has also been developed for the evaluation of soot formation in the reverse flow reformer [22]. This model can be described as a static model of the forced unsteady-state system. The static model is described in brief in Section 2.2.

The static model has been validated against the more extensive dynamic model in previous work, showing that the simplified model gives an accurate description of the reactions taking place during reforming of a producer gas in a reverse-flow POX reactor [22]. A short summary will be presented here. The GRI-mechanism was used within the two models for both simulations. The composition of the gas for these simulations is given in Table 2. The oxygen flow is 6% of the total inlet molar flow and is injected 0.2 m from the gas inlet. The results are presented in Fig. 2. Good agreement between the models can be noted in Fig. 2 and only minor differences between the models could be discerned. It is therefore believed that the static model is able to adequately describe the trends observed in the dynamic model.

2.1. Dynamic model

This model was used to investigate how the reverse flow concept could be applied to reforming a producer gas. The simulations were performed using a C++ program, and a third party library, Cantera, was used to calculate thermodynamics and kinetics. Cantera uses the GRI-Mech 3.0 mechanism for the kinetics [23]. This reaction mechanism was originally designed to model the combustion of natural gas, and has been shown to give results that agree closely with experimental data for reforming processes [6]. However, this mechanism does not include the formation of tars and soot.

The reverse flow reformer is described by a numerical model designed to accurately describe the dynamic behavior of the reactor. The gas phase is modeled as a series of tank reactors. This simplifies the mass balances and the energy balance for the gas phase making the calculations less demanding. The outgoing composition from each reactor is used as the ingoing composition in the following reactor in the reactor series. The solid phase is

Table 1
Dimensions of the modeled reactor.

Property	Value
Reactor length	0.6 (m)
Reactor diameter (thickest)	0.1 (m)
Diameter ratio (max/min)	3

Table 2
Gas composition used for validation of the static model against the dynamic model.

Component	Composition (vol%)
C_2H_4	3.1
CH_4	8.2
CO	11.9
CO_2	27.9
H_2	11.8
H_2O	37.7

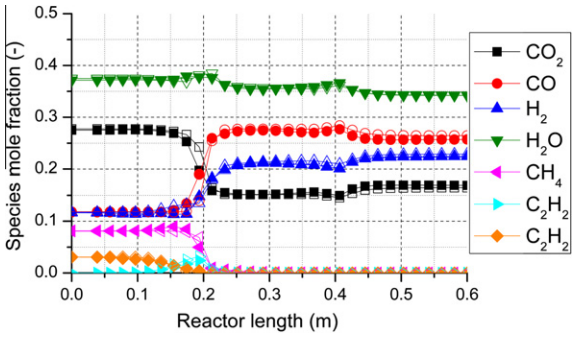

Fig. 2. Comparison of species mole fractions obtained with the detailed and simplified simulation models. Filled symbols represent the dynamic model and empty symbols represent the static model.

modeled with the finite difference method and the partial differential equation describing the solid phase has to be discretised in the space dimension.

For the sake of evaluation, it was necessary to achieve a pseudo-steady-state in the reactor. The time the system is operated in each direction is called the cycle time, and this will vary depending on the conditions in the system. In order to determine when pseudo-steady-state was achieved the temperature profiles of each cycle were evaluated. A deviation of 5 K between the temperature profiles of the cycles was allowed. After five cycles with a temperature difference of 5 K or less the system was considered to be in pseudo-steady-state.

2.2. Static model

For the purpose of studying soot formation the GRI-Mech 3.0 reaction mechanism cannot be used as it does not include higher hydrocarbons and tars. Therefore another reaction mechanism is needed to describe the kinetics in the numerical model. A mechanism that describes conventional gas phase reactions and particle growth was therefore used [24,25]. The mechanism, together with the corresponding thermodynamic and transport property data, is available on-line [26]. This mechanism was developed to describe the formation of polycyclic aromatic hydrocarbons and soot in fuel-rich benzene flames. Because the mechanism that describes soot formation is much larger than the GRI-Mech 3.0 mechanism it was not possible to use it within the dynamic model of the reverse-flow reformer previously described. For this reason, a simplified numerical model was developed for the evaluation of soot formation in the reverse-flow POX reactor [22].

The simplified model can be described as a static model, the principle of which is illustrated in Fig. 3. The model consists of a series of reactors. The reverse-flow reactor is divided into segments and each segment is modeled as a separate reactor. The residence time of each reactor corresponds to the residence time of the reverse-flow reactor segment modeled. The temperature profile over the series of reactors is determined at pseudo-steady-state for each case modeled, using the more extensive dynamic model previously described in Section 2.1. The temperature and pressure in each reactor are kept constant. The composition of the gas leaving each reactor is used as the incoming composition in the following reactor in the series. The oxygen inlet is located 0.2 m from the gas inlet. The solid phase is not included in the model.

2.3. Validation of the static model

Soot formation during the reforming of hydrocarbon fuels has been observed in several experimental studies [5,10,15,16,27]. These mainly concerned the partial oxidation of methane–air mixtures, although ethane and propane have also been studied [15]. The experiments were performed in packed-bed reactors, some operated in reverse-flow mode [15,16]. The formation of higher hydrocarbons was noted in all studies at high equivalence ratios, although the onset of soot formation varied due to differences in the experimental setups. In some cases, the size of the packing material affected soot formation; smaller particles showing less soot formation [5,27]. The bed material itself should be inert and not affect the gas phase reaction. An explanation of a particle-size dependency could be that the void space between the individual particles increases with increasing particle size. When the free distance in the void exceeds the quenching distance for the local gas mixture in question, the gas can be ignited in the void space. This will give rise to a local high temperature in the flame affecting the formation of soot. When the free void distance is less than the quenching distance, the reaction instead proceeds via a homogeneous gas phase reaction.

Soot formation was observed by Valin et al. [10] when reforming a producer-gas-like gas. They investigated the methane conversion of a simulated producer gas during thermal reforming at high temperatures (1273–1773 K) and various residence times. The gas mixture consisted of CO, CO_2, CH_4, H_2 and H_2O. No higher hydrocarbons or tars were included. The experiments were performed in a down-flow isothermal plug-flow reactor, referred to as the PEGASE reactor. The reactor was designed to study the conversion of methane, light hydrocarbons and tars at high temperature. The reactor is heated by Kanthal heating elements and consists of a preheating zone and an isothermal reaction zone. The reacting gas was injected into the reactor and preheated to the desired temperature in the preheating zone before entering the reaction zone. The gas was then cooled to 1173 K and maintained at that temperature until it left the experimental setup [10]. Soot formation was observed during the experiments but not measured quantitatively. However, qualitative comparisons were made regarding the amount of soot formed at various experimental conditions. The results of their study regarding soot formation are summarized in Table 3. A peak in soot formation was observed between 1363 and 1645 K. The hydrogen content of the gas was observed to have considerable influence on the soot formation. More hydrogen in the gas significantly reduced the amount of soot formed. This is in agreement with prior studies reporting that hydrogen represses soot formation due to tar cracking [28,29].

Because of the difficulty in finding experimental data on the reforming of a producer-gas-like gas using a reverse-flow POX reactor it was decided to validate the simplified numerical model, i.e. the static model presented in this work, with the experimental data obtained by Valin et al. for the thermal reforming of producer gas using the PEGASE reactor [10]. The reactor setup described by the numerical model was modified to suit the PEGASE reactor setup, with three reactors representing the preheating zone, the reaction zone and the cooling zone. The main difference between the PEGASE and reverse-flow reactor setups is that the PEGASE reactor is isothermal and is operated unidirectionally.

As a first check of the validity the results for the numerical model was compared to the trends observed by Valin et al. and

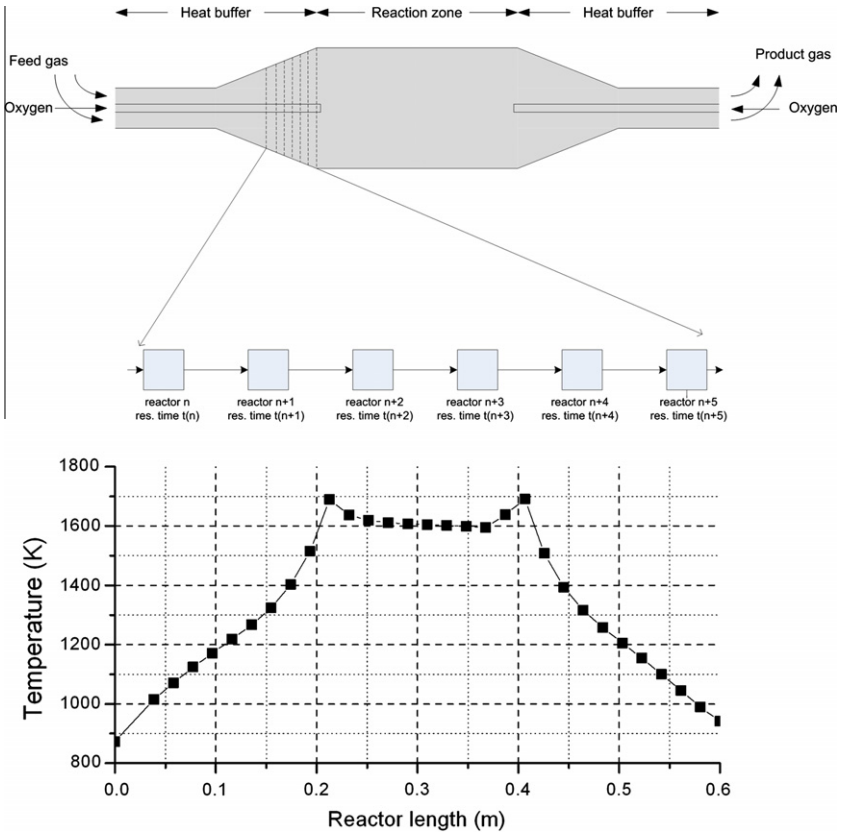

Fig. 3. A schematic description of the series of tanks employed in the model and an example of the temperature profile over the length of the reactor.

Table 3
Soot formation during thermal reforming of bio-syngas according to Valin et al. [10].

	Gas composition (mol%)					Temperature (K)	Residence time (s)	Soot formation
	CO	CO_2	CH_4	H_2	H_2O			
A	19	14	7	16	25	1363–1645	2.1	A peak in soot formation was observed between 1356 and 1645 K.
B	19	14	7	16	25	1783	3.5	Soot formation was relatively low.
C	19	14	7	16	15	1453	2.1	Soot formation was relatively high.
D	19	14	7	32	15	1453	2.1	Soot formation was considerably reduced compared to case C.

summarized in Table 3. The static model showed a peak in soot formation between 1363 and 1645 K with the largest soot formation predicted at 1453 K which corresponds to the observed trend of Valin et al., case A. The predicted soot formation for case B was low and there was a drastic decrease in the predicted soot formation between cases C and D, as was also observed by Valin et al. A simulation of the experimental conditions described by Valin et al. was then conducted and the results obtained with the numerical model were then compared to the experimental data. The results are presented in Fig. 4.

Fig. 4 shows the output gas composition as a function of temperature in the reaction zone. It can be seen that the numerical model shows an overall good correlation with the experimental data. However, at higher temperatures the concentration of CO is underpredicted, and the concentration of H_2O is overpredicted by the numerical model. This may be a consequence of an overprediction of soot formation, in the reaction mechanism used, which results in a loss of carbon. The main reaction controlling the proportions of CO and H_2O is the water gas shift (WGS) equilibrium described below.

$$CO + H_2O \leftrightarrow CO_2 + H_2 \quad (1)$$

If the carbon that is transformed into soot mainly originates from reactions involving CO this concentration would be lowered, shifting the WGS equilibrium to the left. As a result of this, more H_2O would be formed, which would explain the results obtained with the numerical model. The results for the higher hydrocarbons, C_2H_2, C_2H_4 and C_2H_6, are well within the range of those obtained during the experiments, with levels below 0.6% by volume. There does, however, seem to be a slight overprediction of the C_2H_2 in the case of low carbon content in the gas (Fig. 4a) and also in the production of ethane in the high carbon case (Fig. 4b).

It can be concluded from the results obtained with the numerical model that the model will underestimate the CO concentration and overpredict the H_2O concentration at higher temperatures. However, the results for the concentrations of CH_4, CO_2 and H_2 correspond very well with the experimental data over the entire temperature range. The deviations of the model from the experimental data for CO and H_2O occur only at higher temperatures.

In conclusion, the results obtained with the numerical model were found to show good agreement with the experimental data. However, the output of the numerical model should not be interpreted in terms of absolute values but as a basis for the comparison of different operational alternatives.

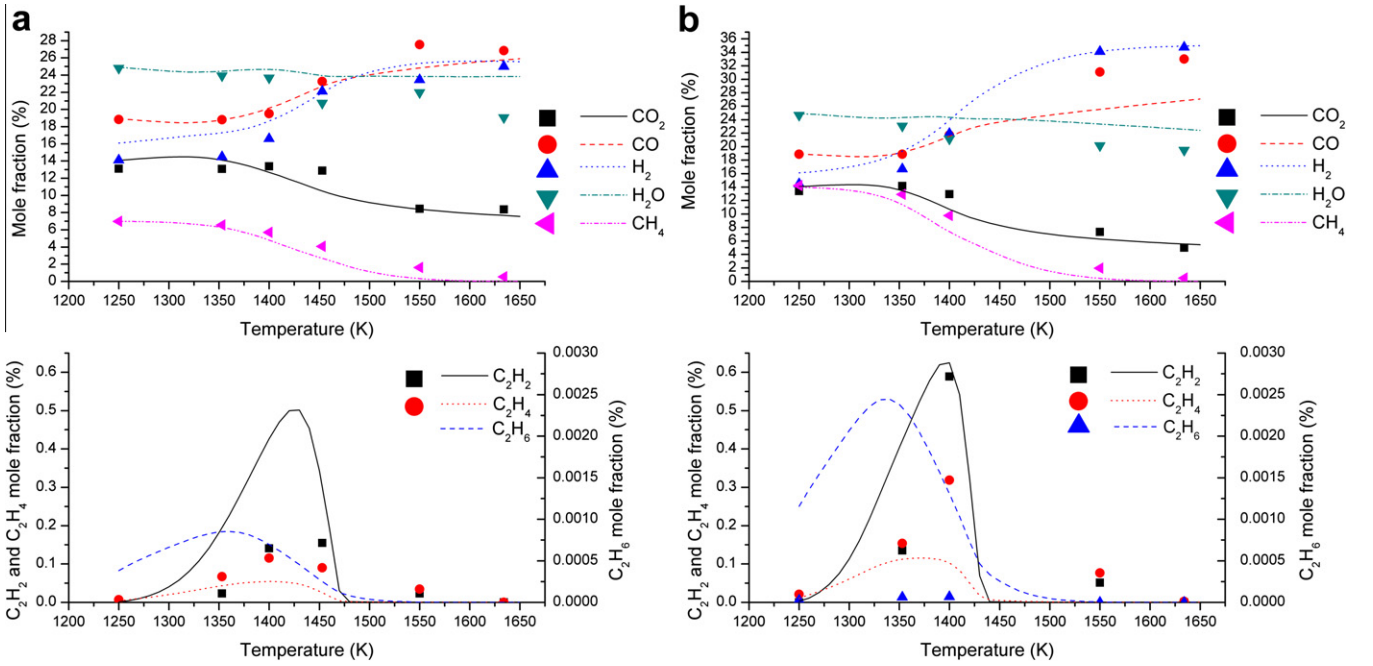

Fig. 4. Concentration profiles in the reactor as a function of temperature with a residence time of 2.1 s. Experimental (symbols) and calculated (lines) values; (a) CH_4: 7 mol% and (b) CH_4: 14 mol% (H_2O: 25 mol%; H_2: 16 mol%; CO: 19 mol%; CO_2: 14 mol% in both cases). Experimental data taken from Valin et al. [10].

3. Simulations

Simulations were performed with varying incoming gas composition in order to determine the extent to which certain species affect soot formation. The results of the simulations were evaluated regarding synthesis gas energy efficiency and methane conversion, as well as soot reduction. As the incoming gas composition was varied the temperature profile over the reactor will also be affected, as well as the amount of oxygen that must be added. Therefore, the temperature profiles for the different cases and the amount of oxygen required in each case were determined prior to the simulations with the dynamic model previously described. All simulations regarding soot formation were performed with the static model described in the modeling section.

One base case was modeled and eight cases with different gas compositions, as summarized in Table 4. The composition of the gas in the base case was chosen to represent a typical composition of a gas leaving a gasifier in terms of CO, CO_2, CH_4, H_2 and H_2O content. The composition from a gasifier depends greatly on the type of gasifier and the operating conditions as well as on which type of biomass is used. In cases 1 and 2 different water contents in the gas were investigated. In case 3 the hydrogen content in the gas was doubled to study the effect of hydrogen on soot formation. As has been observed previously, the hydrogen content has a considerable influence on the amount of soot formed, but it is not known how this will affect the synthesis gas energy efficiency and methane conversion. In cases 4 and 5 the methane content of the gas was studied. The effect of carbon monoxide content in the gas was studied in case 6, and in case 7 the influence of carbon dioxide content on soot formation was investigated. From these simulations it will be possible to deduce which gas component has the greatest influence on soot formation, or whether the total carbon level is more important. In case 8 the effect of tar content was studied. All the naphthalene, the model compound for tar, was assumed to be reformed to ethylene. Both ethylene and naphthalene are known soot precursors but differ in molecular size and structure. In order to determine if it is advantageous to reform the tars present in the producer gas before the reverse flow reformer all the naphthalene was assumed to be reformed to ethylene and the effect of this on the soot formation was determined.

The synthesis gas energy efficiency was calculated according to Eq. 2, where LHV stands for lower heating value.

$$\eta = \mathrm{LHV}_{\mathrm{CO+H2out}}/\mathrm{LHV}_{\mathrm{total\ in}} \quad (2)$$

Table 4
Composition of incoming gas in the modeled cases (mol%) and the amount of oxygen added to the process (mol% of total incoming gas flow).

Component	Base case	1	2	3	4	5	6	7	8
CH_4	7	7	7	7	4	10	7	7	7
C_2H_4	1.5	1.5	1.5	1.5	1.5	1.5	1.5	1.5	4
CO	19	19	19	19	19	19	12	19	19
CO_2	14	14	14	14	14	14	14	24	14
H_2	16	16	16	32	16	16	16	16	16
H_2O	25	15	35	25	25	25	25	25	25
$C_{10}H_8$	0.5	0.5	0.5	0.5	0.5	0.5	0.5	0.5	0
N_2	17	27	7	1	20	14	24	7	15
Added O_2	5	5	5	5	4	5	5	5.5	5.5
Peak temperature (K)	1665	1659	1667	1680	1683	1570	1655	1679	1663
Total carbon (g/m^3)	77	77	77	77	72	82	66	93	77

Table 5
Summary of the results from the cases modeled. Soot formation is given as mass% of the incoming carbon and energy efficiency and methane conversion are given in %.

	Base case	1	2	3	4	5	6	7	8
Soot formation (mass% of incoming carbon)	11.1	11.5	10.7	10.9	10.6	12.2	13.0	8.9	6.6
Synthesis gas energy efficiency	74	73	75	77	75	70	71	76	81
Methane conversion	95	96	95	92	94	97	96	97	94

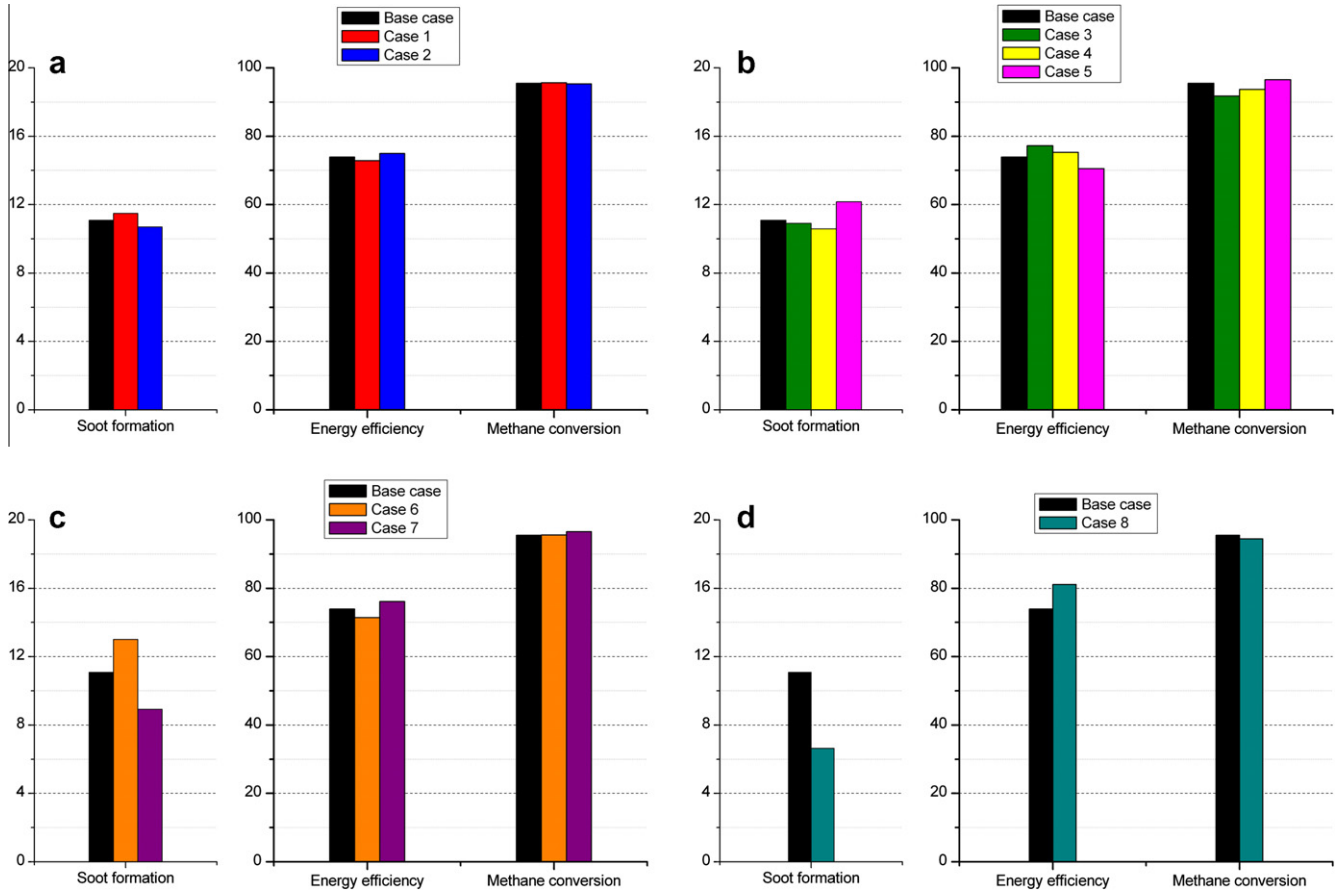

Fig. 5. The results of the cases modeled compared to the base case. Energy efficiency and methane conversion are given in % and the soot formation is given in mass% of the incoming carbon.

The soot formation is reported as the amount of carbon in the soot as a percentage of the incoming total carbon content in the gas. The amount of incoming carbon was not the same in all simulations (Table 4).

4. Results and discussion

The results of the simulations are summarized in Table 5, where the soot formation, synthesis gas energy efficiency and methane conversion are reported. This is also illustrated in Fig. 5. The relatively low synthesis gas energy efficiency is mainly attributed to the, albeit high, but not full, conversion of methane and, of course, to the formation of soot. A substantial amount of energy remains in the unconverted methane. As can be seen in Table 4 the peak temperature differs only slightly between the simulated cases, except for case 5 where the peak temperature is significantly lower due to the high methane content of the gas. Therefore the impact of the peak temperature on the results will probably be negligible, except for case 5.

Not surprisingly, lowering the water content of the gas (case 1) increased the amount of soot formed and increasing the water content of the gas (case 2) showed a slight decrease in soot formation, see Fig. 5a. However, the effect of water content on the soot formation was not as significant as anticipated. It appears that, at the concentrations studied, the water content of the gas has only a minor effect on the amount of soot formed. The synthesis gas energy efficiency and methane conversion for these alternatives were also insignificantly reduced with higher water content (case 2).

Soot formation is reduced, compared with the base case, in case 3 (increased H_2 content) and case 4 (reduced methane content), see Fig. 5b. This is consistent with previous findings that increasing the hydrogen content of the gas reduces soot formation [28,29], and also that methane seems to have a negative effect on soot formation, as in case 5 (increased methane content). However, the increase in hydrogen content in the gas did not affect the soot formation as much as expected but only shows slightly lower soot formation compared to the base case. Since the hydrogen content in the gas was doubled, the effect on soot formation was expected to be higher. Instead the hydrogen content only seems to have a minor effect on the amount of soot formed in the reverse flow reformer. In order to determine the cause of this minor effect further investigations are necessary. For case 5 the soot formation is

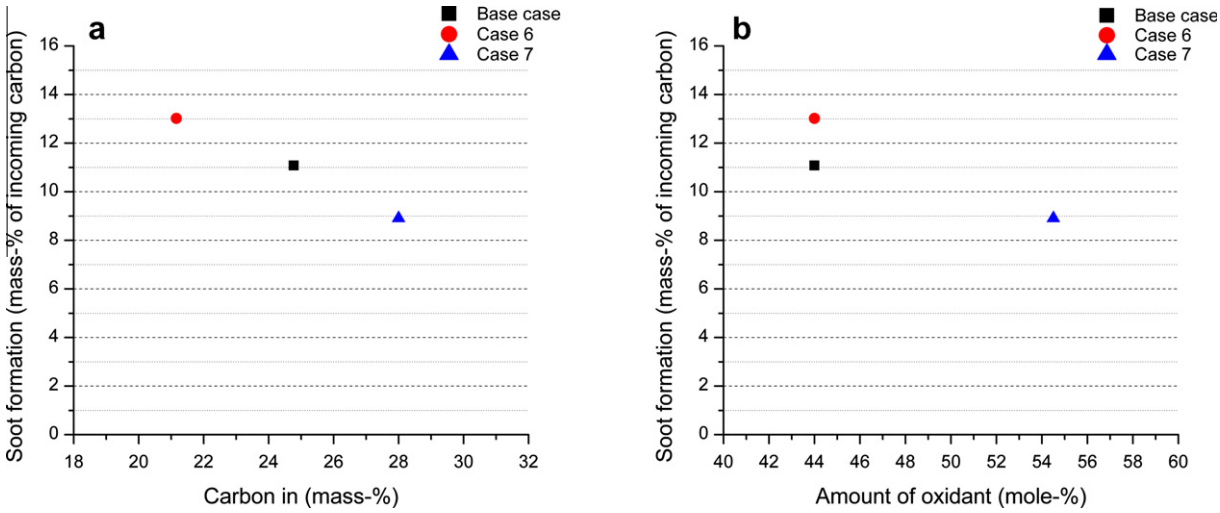

Fig. 6. Soot formation as a function of the amount of carbon (a) and amount of oxidant (b) for each case modeled. The amount of oxidant is the combined amount of O_2, CO_2 and H_2O. Square symbols represent the base case, circles represent case 6 and triangles represent case 7.

increased and the synthesis gas energy efficiency is decreased. This is most likely due to the lower peak temperature for this case (see Table 4). Both synthesis gas energy efficiency and methane conversion are of course greatly affected by varying the methane and hydrogen content of the gas.

In the cases with less CO and more CO_2 in the gas (cases 6 and 7) shown in Fig. 5c, it was found that decreasing the CO content of the gas gave rise to an increase in the amount of soot formed. The opposite was observed when the CO_2 content of the gas was increased, as has been reported previously [22]. This is not surprising since it is well known that CO_2 can act as an oxidizing agent in this type of reaction, donating oxygen and thus forming CO [30,31]. Both the synthesis gas energy efficiency and methane conversion were increased in case 7. Case 6 has the lowest concentration of CO in the outgoing gas and case 7 has the highest. It appears that the concentration of CO in the outgoing gas is somehow correlated to the amount of soot formed. This is believed to be connected to the addition of CO_2 as it will act as an additional oxidation agent (forming CO) and thus increase the oxidation potential of the gas mixture, which will further suppress the soot formation. However, the amount of incoming carbon is not the same in all cases (see Table 4). It may, therefore, be more correct to take this into account when the results are discussed. The amount of incoming carbon is lower in case 6, compared to the base case, and significantly higher for case 7, compared to the base case. If the actual mass of soot formed, i.e. the mass% (given in Table 5) times the total amount of carbon in (given in Table 4), is compared instead, it can be seen that the mass of soot formed is almost the same for case 6 and the base case (8.55 g/m^3 and 8.57 g/m^3 respectively). The mass of soot formed for case 7 is somewhat lower (8.30 g/m^3). The results from these cases were further investigated in Fig. 6. In Fig. 6a it can be seen that the amount of soot formed decreases as the carbon content in the incoming gas increases. In terms of the actual amount of soot formed this is not entirely true as the mass of soot is almost the same for the base case and case 6. In case 7 the mass of soot formed is somewhat lower than that for the base case and case 6. In Fig. 6b it can also be seen that the amount of oxidant (O_2, CO_2 and H_2O) in case 7 is higher than in case 6 and the base case, due to a larger addition of oxygen and a higher CO_2 content (see Table 4). This indicates that the amount of oxidant in each case may be the dominating factor controlling the amount of soot formed. Fig. 6 also shows that the amount of oxidant is not the sole factor affecting soot formation; the kinetics will of course also play an important role in the amount of soot formed.

For case 8, depicted in Fig. 5d, the soot formation was considerably reduced. For this case a slightly higher amount of oxygen was added (see Table 4) which will also influence the results to some extent. However, the higher amount of oxygen added in this case is only part of the explanation and most of the reduction will be due to the fact that no tars are present in the gas. The synthesis gas energy efficiency of the process was greatly improved for case 8, mainly due to the lower amount of energy bounded in the soot formed. The methane conversion was somewhat lower in this case. The results clearly show that the more large soot precursors that are present in the gas, the more soot will be formed. It is therefore of great interest to further study ways of cracking the tars in the producer gas in an energy efficient way before reforming the methane and C_2-hydrocarbons.

5. Conclusions

The aim of this investigation was to examine the extent to which soot is likely to form and possible ways of reducing soot formation. One base case and eight cases with different gas compositions were simulated and studied. The results were evaluated from the viewpoint of synthesis gas energy efficiency and methane conversion, as well as soot reduction. The results showed that neither the steam nor the hydrogen content of the gas affected the soot formation to any high degree, which was unexpected. The methane content of the gas had a greater impact on the amount of soot formed. The amount of soot formed was reduced when more CO_2 was present in the incoming gas, probably due to the increased amount of oxidant present. The synthesis gas energy efficiency and methane conversion were also positively affected by increasing the concentration of CO_2. The best results regarding soot formation were obtained for the case in which no tars were present in the incoming gas.

The reaction mechanism used in the numerical model presented in this work was not developed to describe reforming, but was designed to describe the combustion of benzene in fuel-rich flames. Theoretically, the model should also be valid for reforming, but the deviation from expected behavior may indicate that it does not adequately describe the reactions involved. It would therefore

be of interest to develop a reaction mechanism that describes soot formation in reducing environments such as reforming.

From the results obtained it was concluded that in order to reduce the amount of soot formed in the reverse-flow POX reactor studies should be carried it to further study ways of reducing the amount of tars in the gas in an energy efficient way. Experimental research on this process is under way and will be presented in a later publication.

Acknowledgements

The authors are grateful to the European Commission for financial support within the framework of the FP7 Integrated Project "GreenSyngas" (Project No. 213628). We would also like to thank the Swedish Energy Agency (STEM) and E.ON for their financial support.

References

[1] Hamelinck CN, Faaij APC, den Uil H, Boerrigter H. Production of FT transportation fuels from biomass; technical options, process analysis and optimisation, and development potential. Energy (Amsterdam, Neth.) 2004;29:1743–71.
[2] Buragohain B, Mahanta P, Moholkar VS. Thermodynamic optimization of biomass gasification for decentralized power generation and Fischer–Tropsch synthesis. Energy 2010;35:2557–79 [Oxford, UK].
[3] James OO, Mesubi AM, Ako TC, Maity S. Increasing carbon utilization in Fischer–Tropsch synthesis using H_2-deficient or CO_2-rich syngas feeds. Fuel Process Technol 2010;91:136–44.
[4] Manganaro J, Chen B, Adeosun J, Lakhapatri S, Favetta D, Lawal A, et al. Conversion of residual biomass into liquid transportation fuel: an energy analysis. Energy Fuels 2011;25:2711–20.
[5] Al-Hamamre Z, Vosz S, Trimis D. Hydrogen production by thermal partial oxidation of hydrocarbon fuels in porous media based reformer. Int J Hydrogen Energy 2009;34:827–32.
[6] Dufour A, Valin S, Castelli P, Thiery S, Boissonnet G, Zoulalian A, et al. Mechanisms and kinetics of methane thermal conversion in a syngas. Ind Eng Chem Res 2009;48:6564–72.
[7] Peña MA, Gomez JP, Fierro JLG. New catalytic routes for syngas and hydrogen production. Appl Catal A 1996;144:7–57.
[8] Albertazzi S, Basile F, Brandin J, Einvall J, Hulteberg C, Fornasari G, et al. The technical feasibility of biomass gasification for hydrogen production. Catal Today 2005;106:297–300.
[9] CHRISGAS. Clean hydrogen-rich synthesis gas – fuels from biomass. Intermediate report, Swedish Energy Agency, Växjö; 2008.
[10] Valin S, Cances J, Castelli P, Thiery S, Dufour A, Boissonnet G, et al. Upgrading biomass pyrolysis gas by conversion of methane at high temperature: experiments and modelling. Fuel 2009;88:834–42.
[11] Albertazzi S, Basile F, Barbera D, Benito P, Brandin J, Einvall J, et al. Deactivation of a Ni-based reforming catalyst during the upgrading of the producer gas, from simulated to real conditions. Top Catal 2011;54:746–54.
[12] Albertazzi S, Basile F, Brandin J, Einvall J, Fornasari G, Hulteberg C, et al. Effect of fly ash and H_2S on a Ni-based catalyst for the upgrading of a biomass-generated gas. Biomass Bioenergy 2008;32:345–53.
[13] Christensen TS. Adiabatic prereforming of hydrocarbons – an important step in syngas production. Appl catal A. Gen 1996;138:285–309.
[14] Jens S. Four challenges for nickel steam-reforming catalysts. Catal Today 2006;111:103–10.
[15] Toledo M, Bubnovich V, Saveliev A, Kennedy L. Hydrogen production in ultrarich combustion of hydrocarbon fuels in porous media. Int J Hydrogen Energy 2009;34:1818–27.
[16] Drayton MK, Saveliev AV, Kennedy LA, Fridman AA, Li Y.-E. Syngas production using superadiabatic combustion of ultrarich methane-air mixtures. In: 27th Symp. (Int.) Combust., Proc.; 1998. p. 1361–7.
[17] Weinberg FJ, Bartleet TG, Carleton FB, Rimbotti P, Brophy JH, Manning RP. Partial oxidation of fuel-rich mixtures in a spouted bed combustor. Combust Flame 1988;72:235–9.
[18] Tunå P, Svensson H, Brandin J. Modeling of reverse flow partial oxidation process for gasifier product gas upgrading. In: 5th International conference on thermal energy: theory and applications, Marrakesh, Morocco; 2010.
[19] Kennedy IM. Models of soot formation and oxidation. Prog Energy Combust Sci 1997;23:95–132.
[20] Frenklach M. Reaction mechanism of soot formation in flames. Phys Chem Chem Phys 2002;4:2028–37.
[21] Richter H, Howard JB. Formation of polycyclic aromatic hydrocarbons and their growth to soot – a review of chemical reaction pathways. Prog Energy Combust Sci 2000;26:565–608.
[22] Svensson H, Tunå P, Brandin J. Soot formation in reverse flow reforming of biomass gasification producer gas. In: Proceedings of 18th European biomass conference and exhibition. ETA-florence reneweble energies/WIP-renewable energies, Lyon, France; 2010.
[23] Frenklach M, Bowman T, Smith G, Gardiner B. <http://www.me.berkeley.edu/gri_mech/index.html, in>.
[24] Ergut A, Granata S, Jordan J, Carlson J, Howard JB, Richter H, et al. PAH formation in one-dimensional premixed fuel-rich atmospheric pressure ethylbenzene and ethyl alcohol flames. Combust Flame 2006;144:757–72.
[25] Richter H, Granata S, Green WH, Howard JB. Detailed modeling of PAH and soot formation in a laminar premixed benzene/oxygen/argon low-pressure flame. Proc Combust Inst 2005;30:1397–405.
[26] J.B. Howard, et al. <http://web.mit.edu/anish/www/MITcomb.html>.
[27] Gavrilyuk VV, Dmitrienko YM, Zhdanok SA, Minkina VG, Shabunya SI, Yadrevskaya NL, et al. Conversion of methane to hydrogen under superadiabatic filtration combustion. Theor Found Chem Eng 2001;35:589–96.
[28] van der Hoeven TA, de Lange HC, van Steenhoven AA. Analysis of hydrogen-influence on tar removal by partial oxidation. Fuel 2006;85:1101–10.
[29] Houben MP, de Lange HC, van Steenhoven AA. Tar reduction through partial combustion of fuel gas. Fuel 2005;84:817–24.
[30] Ginsburg JM, Piña J, El Solh T, de Lasa HI. Coke formation over a nickel catalyst under methane dry reforming conditions: thermodynamic and kinetic models. Ind Eng Chem Res 2005;44:4846–54.
[31] Valderrama G, Kiennemann A, Goldwasser MR. Dry reforming of CH_4 over solid solutions of $LaNi_{1-x}Co_xO_3$. Catal Today 2008;133–135:142–8.